J. Fluid Mech. (1971), *vol.* 49, *part* 4, *pp.* 657–691
Printed in Great Britain

A pulsed-wire technique for velocity measurements in highly turbulent flows

By L. J. S. BRADBURY† AND I. P. CASTRO
Aeronautics Department, Imperial College

(Received 8 January 1969 and in revised form 24 September 1970)

The velocity measuring technique described in this paper consists of measuring the time of flight of a tracer of heated air from an electrically pulsed wire to one of two sensor wires which are operated as resistance thermometers. These sensor wires are at right angles to the pulsed wire and are placed one on either side of the pulsed wire. The instrument may be used in highly turbulent flows including regions in which flow reversals occur. The paper discusses the theoretical behaviour of the probe and the results of some calibration experiments.

1. Introduction

In a highly turbulent flow, instruments such as hot-wire anemometers and pitot-static tubes used for velocity measurements are subject to serious errors. This is due not only to the non-linear response of these instruments to fluctuations in the magnitude of the velocity vector, but also to their ambiguous response to variations in the flow direction. This paper describes a measuring technique which largely avoids these difficulties, and which can be used in highly turbulent flows including flow regions in which reversals of the flow direction occur. The technique is similar to that described by Bauer (1965) in which two fine platinum wires of $2{\cdot}5\,\mu$ diameter mounted on hot-wire probes were used. These were placed parallel to one another with one wire downstream of the other. A tracer of heated air was introduced into the flow by pulsing the upstream wire with a voltage pulse of a few microseconds duration and the time taken for this tracer to reach the downstream wire was measured using the downstream wire as a simple resistance thermometer. This parallel-wire arrangement is very sensitive to flow direction and, in a turbulent flow, many of the heat pulses would miss the resistance wire altogether. However, by the simple expedient of placing the sensor wire at right angles to the pulsed wire, it is possible to produce an instrument with a wide yaw response which can be used in a highly turbulent flow. The aim of the present paper is to discuss the behaviour of such an instrument, and to draw more attention to the technique, which seems to have considerable potential for making measurements in highly turbulent flows under precisely the conditions where the hot-wire anemometer even in its linearized form is suffering seriously from errors due to its ambiguous yaw response.

Early work on this technique has already been discussed by Bradbury (1969)

† Present address: Mechanical Engineering Department, University of Surrey.

and some similar work has also been carried out by Tombach (1969). However, there are some important differences between Tombach's work and the present investigations, which greatly influence the usefulness of the technique. These differences will be discussed in § 5 after the details of the present work have been described.

2. Theoretical considerations

2.1. *The ideal response of a crossed-wire probe*

The probe under consideration consists of three wires (figure 1). The central wire is the pulsed wire and on either side of this are the sensor wires with their axes perpendicular to the pulsed-wire axis. Before considering the real behaviour of

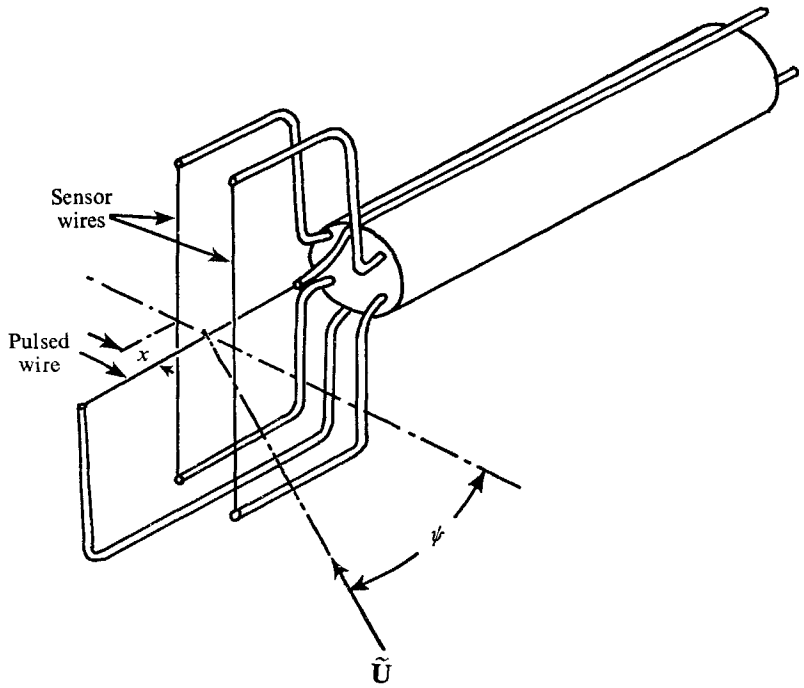

FIGURE 1. Sketch of a pulsed-wire probe.

such a probe, it is useful to describe the ideal response that would give unambiguous measurements of velocity. In an ideal probe, the pulsed-wire temperature would jump instantaneously from ambient temperature to some much higher temperature and be held there while the resultant tracer of heated air was convected away with the instantaneous velocity of the stream passing the probe. If both thermal and viscous diffusion effects were small, the time taken for the front of the tracer to reach a sensor wire would be $t = x/(|\mathbf{U}| \cos\psi)$ where x is the distance between the pulsed and sensor wires and ψ is the angle between the direction normal to the plane of the probe and the instantaneous velocity vector $\mathbf{U}$ (see figure 1). The plane of the probe is defined here as the plane parallel to all three wires in the probe. Thus, from the time of flight, the magnitude of the

velocity vector resolved at right angles to the plane of the probe could be obtained. The use of two sensor wires, one on either side of the pulsed wire, would ensure that the direction of the flow at that instant could be unambiguously determined; the only restriction would be in the length l of the wires since $\tan^{-1}(l/2x)$ gives the largest angular deviation of the flow direction that could be sensed by the probe. In the probes to be described later on, l/x was about 5 giving a maximum flow deflexion angle of about 70°. If a sufficient number of these time of flight measurements were made at a particular station then the technique would give both the mean and fluctuating components of velocity in the direction at right angles to the plane of the probe, and velocities in any direction could be studied simply by aligning the probe in that direction. The only other restriction on the probe would be that it would not properly respond to turbulent fluctuations which had a length scale appreciably less than the probe dimensions.

With this brief description of an ideal probe response, we can now look at the real response in some detail. Bauer has considered some aspects of the behaviour of the pulsed-wire technique but some further elaboration is needed because the behaviour of the crossed-wire probe is different from the parallel-wire probe in a number of important ways. The analysis is restricted to a flow which is steady during the time of flight of the heat tracer, and the object of the analysis is to highlight the influence of the various parameters that arise in the problem. It is worth pointing out that the results of the analysis are not necessary for the practical application of the technique in much the same way as detailed knowledge of the heat-transfer laws for fine wires is not necessary in the more usual application of constant-temperature hot-wire anemometers. However, in order to exploit fully measurement techniques of this sort, it is clearly important to study the influence of the various parameters involved.

In § 2.2 the temperature variation with time of the pulsed wire is considered. Then, in § 2.3 the temperature field produced downstream of the pulsed wire and the response of the sensor wire to it are considered for the case in which thermal diffusion is neglected. The important modification to these results from thermal diffusion is then examined in § 2.4. Attention is then given in § 3 to the practical problems of applying the technique and results of calibration experiments are discussed in § 4. Finally, in §§ 5 and 6, the results of measurements in highly turbulent flows are described.

2.2. *The temperature variation of the pulsed wire*

The suffix notation used in the following discussion is as follows. The suffices f and w refer to properties of the flow and wire respectively. However, in the case of the wires, if the properties refer specifically to either the pulsed or sensor wire, the suffix w will be replaced by either p or s as the case may be.

The temperature variation of both the pulsed wire and sensor wires can be studied from the equation

$$\underbrace{\frac{V^2}{r}}_{\substack{\text{Electrical}\\ \text{heating}}} = \underbrace{\rho_w c_w \frac{\pi d^2 l}{4}\frac{d\theta_w}{dt}}_{\substack{\text{Heat stored}\\ \text{in wire}}} + \underbrace{\pi k_f l N_w(\theta_w - \theta_f)}_{\substack{\text{Heat convection}\\ \text{by stream}}}, \tag{1}$$

where θ_w, θ_f are the wire and flow temperatures respectively; d is the wire diameter and l its length, ρ_w and c_w are the density and specific heat of the wire material; r is the wire resistance, V the voltage across the wire, N_w the Nusselt number and k_f the thermal conductivity of the gas flowing past the wire. The appropriate temperature at which this thermal conductivity is evaluated depends on the particular heat-transfer law that is chosen. Because of the variety of such laws that are available, some experimental investigations into heat-transfer laws were carried out. These are reported in a separate paper (Bradbury & Castro 1971), but the conclusion arising from this work is that it is sufficient for the calculation of convective time constants – which is, in fact, the only use made of the law in the present paper – to use a simple law in which fluid properties are evaluated at ambient temperature. The actual form of law used is the expression proposed by Collis & Williams (1959) without any wire temperature loading term included. Under these circumstances and at the Reynolds numbers encountered in the present experiments, their relationship is

$$N_w = 0{\cdot}24 + 0{\cdot}56R^{0{\cdot}45}, \tag{2}$$

where $R = Ud/\nu$ is the wire Reynolds number. All experimental heat-transfer laws are derived from steady-state heat-transfer measurements, but it is usually assumed that they will apply to unsteady flows provided $\tau U/d \gg 1$ where τ is the characteristic time for the unsteady flow. This condition is always fulfilled in the present experiments.

In the experiments to be described later, the pulsed wire was subjected to an essentially constant voltage pulse with a duration of only several microseconds which is much less than the time constant for appreciable convection

$$T_p' = \rho_p c_p d^2/(4k_f N_p).$$

Under these circumstances, heat convection can be ignored and the temperature rise of the wire from equation (1) is given by

$$(V/l)^2 \hat{t} = \rho_p c_p \sigma_p \theta_p (1 + \tfrac{1}{2}\alpha\theta_p + \tfrac{1}{3}\beta\theta_p^2), \tag{3}$$

where α and β are the first and second temperature coefficients of resistance respectively which it is necessary to include because of the very high temperatures reached. σ_p is the wire resistivity at some reference temperature which, for convenience, we may take as ambient temperature rather than 0 °C. All other temperatures and properties are also measured relative to ambient temperature. $\hat{t}$ is the duration of the voltage pulse.

After the almost impulsive rise of temperature, the pulsed-wire temperature decays exponentially due to heat convection.

$$\theta_p/\theta_{p_i} = \exp(-t/T_p'), \tag{4}$$

where θ_{p_i} is the wire temperature at the end of the voltage pulse and T_p' is the pulsed-wire convection time constant.

2.3. *The temperature downstream of the pulsed wire and the sensor wire response neglecting the influence of thermal diffusion*

From the point of view of the temperature distribution produced by the pulsed wire, we can regard the pulsed-wire temperature variation as consisting of an instantaneous increase of temperature to the value given by equation (1) followed by the exponential decay with the convective time constant of the wire T_p. If we neglect for the moment the influence of thermal diffusion in smearing out the sharp front of the heat tracer, we have that the heat being convected away by the stream at a distance x from the pulsed wire is equal to the heat flow released from the pulsed wire at an interval of time equal to x/U earlier and it is given by

$$Q = N_p k_f \pi \theta_p = \rho_f c_f U \int_{-\infty}^{\infty} \theta_f dy, \tag{5}$$

where θ_f is the fluid temperature downstream of the pulsed wire, and where it is assumed that the velocity is everywhere equal to the free-stream velocity U. This neglect of the viscous wake will be discussed later with the experimental results. From (4) and (5), the integrated temperature distribution downstream of the pulsed wire in a convenient non-dimensional form is given by

$$\frac{\int_{-\infty}^{\infty} \theta_f dy}{\theta_p x} = \frac{\pi N_p}{P} \exp\left(-\frac{t - x/U}{T_p}\right) H\left(\frac{x}{U}\right), \tag{6}$$

where P is the Péclet number, Ux/κ, and $H(x/U)$ is a Heaviside step function. We can now consider the sensor-wire response to this temperature field.

The sensor wire is operated as a simple resistance thermometer and the constant current passing through it is sufficiently small to enable the electrical heating term in equation (1) to be neglected. When the tracer of heated air arrives, there will be an output voltage from the sensor wire given by

$$\frac{i\alpha r}{l} \int_{-l/2}^{+l/2} \theta_s(y)\, dy, \tag{7}$$

where i is the constant current, r and l are the wire resistance and length respectively and $\theta_s(y)$ is the variation of sensor wire temperature over its length. If the sensor wire is much longer than the width of the heat tracer, we have from equation (1), for the relation between the flow and sensor-wire temperature

$$\int_{-l/2}^{+l/2} \theta_s dy \approx \int_{-\infty}^{\infty} \theta_s dy = \frac{e^{-t/T_s}}{T_s} \int_0^t e^{t/T_s} \left[\int_{-\infty}^{\infty} \theta_f dy\right] dt, \tag{8}$$

where T_s is the sensor-wire time constant. It has been assumed so far that conduction along the length of the wires is not important. As will be discussed later on, the half width of the thermal wake is $\delta = O(2(\kappa_f x/U))^{\frac{1}{2}}$. The time for appreciable conduction is therefore $O(\delta^2/4\kappa_w)$ and, if conduction is to be neglected, this time must be much longer than the sensor-wire time constant, T_s. This reduces to the condition that $(P/16N_s)\,(k_w/k_f)\,(d_s/x)^2$ must be much less than unity.

But, in practice, this quantity has values between about 0·1 and 0·7 so that the influence of conduction along the wires may not necessarily be negligible. However, although the temperature distribution may be affected by conduction, it is easy to show that the integral of the temperature over the length of the wire is not affected so that (8) is not in error due to conduction effects.

Using (6) in (8) we obtain

$$\frac{\int_{-\infty}^{\infty}\theta_s dy}{\theta_{p_i}x} = \frac{\pi N_p}{P}\frac{T_p}{T_p-T_s}\left[\exp\left(-\frac{t-x/U}{T_p}\right)-\exp\left(-\frac{t-x/U}{T_s}\right)\right]H\left(\frac{x}{U}\right), \tag{9}$$

when $T_p \neq T_s$.† This equation gives the response of a sensor wire to a sharp-fronted pulse which subsequently decays in an exponential manner. A rather obvious point is that it shows that the sensor-wire signal does not depend on the distance x between the pulsed wire and the sensor wire except in so far as the time of flight is affected. This is simply a consequence of the conservation of heat, i.e. for a uniform flow velocity, $\int_{-\infty}^{\infty}\theta_f dy$ does not depend on the wire spacing.

The response of the sensor wire shows a discontinuity in slope at time $t = x/U$ with an initial value in non-dimensional terms given by

$$\frac{x^2}{\kappa}\frac{d}{dt}\left[\frac{\int_{-\infty}^{\infty}\theta_s dy}{\theta_{p_i}x}\right] = \pi N_p \frac{x}{UT_s}. \tag{10}$$

The signal also has a maximum value given by

$$\left[\frac{\int_{-\infty}^{\infty}\theta_s dy}{\theta_{p_i}x}\right]_{\max} = \frac{\pi N_p}{P}\left(\frac{T_p}{T_s}\right)^{-T_s/(T_p-T_s)} \tag{11}$$

which occurs at time

$$\frac{t}{T_s} = \frac{T_p}{T_p-T_s}\log\frac{T_p}{T_s}+\frac{x}{UT_s}. \tag{12}$$

Thus, in the absence of diffusion, there would be no difficulty in determining the time of flight because of the discontinuity in slope at $t = x/U$, and, in particular, if the signal were differentiated, this would exhibit a step rise at $t = x/U$ which could be used to trigger an electronic comparator to obtain the time of flight. Before considering the vital question of how diffusion alters these results, one further point should be noted. If we assume roughly that the wire Nusselt number $N \sim R^{0.45}$, the amplitude of the sensor-wire signal shows a variation with free-stream velocity that is like $U^{-0.55}$, so that over, say, a 20 : 1 speed range, there is a variation in signal level of about 5·2 : 1. By contrast, the initial slope of the sensor-wire signal varies more slowly, like $U^{-0.1}$, so that if differentiated signals were used, the amplitude variation would be much less than that of the original signals, and this has an important bearing on possible ways of recording the time of flight, as will be discussed later.

† If $T_p = T_s$, a somewhat different expression is obtained.

2.4. *The influence of thermal diffusion on the sensor-wire signals*

The influence of thermal diffusion can be studied by using solutions of the equation for the convection and diffusion of heat in a stream, namely

$$\frac{\partial\theta_f}{\partial t}+U\frac{\partial\theta_f}{\partial x}=\kappa\left(\frac{\partial^2\theta_f}{\partial x^2}+\frac{\partial^2\theta_f}{\partial y^2}\right). \tag{13}$$

It is again assumed that the velocity is everywhere equal to the free-stream velocity. By introducing the variable $X = x - Ut$ in place of x, the ordinary heat-conduction equation is recovered whose solution can be compounded of simple point heat sources. Thus, the solution of (13) for the thermal wake produced by a pulsed wire with an exponentially decaying temperature is given by

$$\frac{\theta_f(x,y,t)}{\theta_{p_i}}=\frac{N_p}{4}\int_0^{Ut}\frac{\exp\left(-\dfrac{t-x'/U}{T_p}\right)\exp\left(-\dfrac{U}{4\kappa x'}y^2\right)\exp\left(-\dfrac{U(x-x')^2}{4\kappa x'}\right)}{x'}dx'. \tag{14}$$

This integral has a convenient asymptotic behaviour given by

$$\frac{\theta_f(x,y,t)}{\theta_{p_i}}\sim\frac{N_p}{2}\left(\frac{\pi}{P}\right)^{\frac{1}{2}}\exp\left(-\frac{t-x/U}{T_p}\right)\exp\left(-\tfrac{1}{4}P\left(\frac{y}{x}\right)^2\right)\times\left[\frac{\operatorname{erf}(\frac{1}{4}P)^{\frac{1}{2}}-\operatorname{erf}[(\frac{1}{4}P)^{\frac{1}{2}}(1-tU/x)]}{1+\operatorname{erf}(\frac{1}{4}P)^{\frac{1}{2}}}\right], \tag{15}$$

which requires that the Péclet number

$$P = Ux/\kappa \gg 1, \quad (y/x)^2 \ll \tfrac{1}{4}P \quad \text{and} \quad T_p \gg 2x/(UP^{\frac{1}{2}}).$$

The physical interpretation of this solution is that when $P \gg 1$, longitudinal diffusion is significant only near the front of the pulse and it is this term in (13) which gives rise to the functions containing erfs in (15). As discussed by Bauer (1965), this function is like a step function with a rise time of $4x/(UP^{\frac{1}{2}})$. In this time, the rise is about 90 % complete. Away from the front of the pulse, lateral diffusion dominates, and the solution in this region tends to

$$\frac{\theta_f(x,y,t)}{\theta_{p_i}}\sim\frac{N_p}{2}\left(\frac{\pi}{P}\right)^{\frac{1}{2}}\exp\left(-\frac{t-x/U}{T_p}\right)\exp\left(-\tfrac{1}{4}P\left(\frac{y}{x}\right)^2\right), \tag{16}$$

which is the 'quasi-steady' boundary-layer solution of (13) without the longitudinal diffusion term. The solution is quasi-steady because the pulsed-wire temperature is decaying exponentially, and for this solution to be valid, it is necessary that the pulsed-wire time constant should be much longer than the time for appreciable diffusion, i.e. $T_p \gg 2x/(UP^{\frac{1}{2}})$.

In the case of an unyawed probe, the integral of the flow temperature may be obtained from (15) to give

$$\frac{\int_{-\infty}^{\infty}\theta_f dy}{\theta_{p_i}x}=\frac{\pi N_p}{P}\exp\left(-\frac{t-x/U}{T_p}\right)\left[\frac{\operatorname{erf}(\frac{1}{4}P)^{\frac{1}{2}}-\operatorname{erf}[(\frac{1}{4}P)^{\frac{1}{2}}(1-tU/x)]}{1+\operatorname{erf}(\frac{1}{4}P)^{\frac{1}{2}}}\right]. \tag{17}$$

This result differs from the earlier expression without longitudinal diffusion (equation (6)) only by the step-like erf function and it is a result that one might well have written down intuitively without the necessity of the foregoing analysis.

Substituting in (8) for the sensor-wire response, we now obtain the following expression for $T_p \neq T_s$:

$$\frac{\int_{-\infty}^{\infty} \theta_s dy}{\theta_{p_i} x} = \frac{\pi N_p}{P(1+\operatorname{erf}\chi)} \frac{T_p}{T_p - T_s} \left\{ \exp\left(-\frac{t-x/U}{T_p}\right) \left[\operatorname{erf}\chi - \operatorname{erf}\chi\left(1-\frac{tU}{x}\right)\right] \right.$$
$$\left. - \exp\left(-\frac{t-x/U}{T_s}\right) \exp\left[\left(\frac{\lambda x}{2\chi U}\right)^2\right] \left[\operatorname{erf}\left(\chi + \frac{\lambda x}{2\chi U}\right) - \operatorname{erf}\left(\chi\left(1-\frac{tU}{x}\right) + \frac{\lambda x}{2\chi U}\right)\right]\right\}, \tag{18}$$

where $\chi = (\frac{1}{4}P)^{\frac{1}{2}}$, $\lambda = (1/T_s) - (1/T_p)$. This expression is useful because it enables the sensor-wire response to be studied with all the main physical parameters included with the exception of the influence of the pulsed-wire viscous wake.

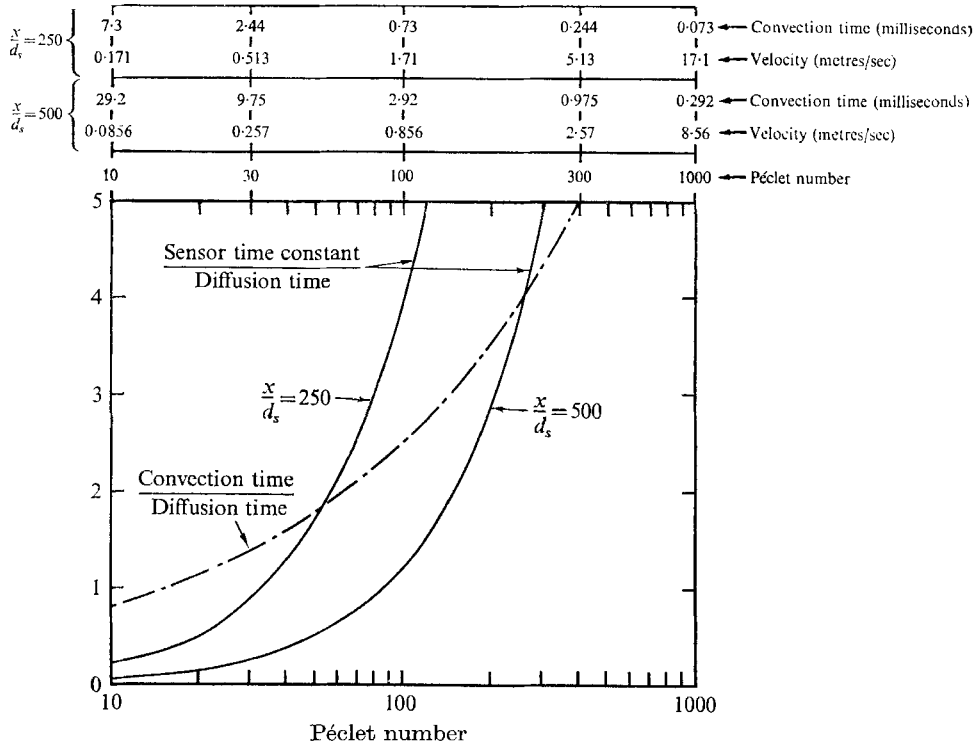

FIGURE 2. Characteristic times of pulsed-wire probes.

However, the interpretation which is put upon the expression depends on the relative magnitudes of the various characteristic times. These characteristic times are (i) the convection time, $T_c = x/U$, (ii) the time taken for the diffusive front to pass, $T_d = 4x/(UP^{\frac{1}{2}})$, (iii) the sensor-wire time constant, $T_s = (\rho_s c_s d^2)/(4k_f N_s)$, (iv) the pulsed-wire time constant, T_p. At this stage, it is pertinent to consider examples of typical probes in order to establish practical values of these characteristic times. The probes used in the majority of the experiments consisted of a pulsed wire of 10μ diameter and a sensor wire of 5μ diameter. The spacing between them varied typically from 1·25 mm to 2·5 mm and figure 2 shows the

ratios of these time constants to one another for these two spacings which are equal to values of x/d_s of 250 and 500 respectively. The results are given as a function of Péclet number, but, in order to give some idea of the real times involved, two additional abscissa scales are shown in which the velocity and convection times for the two typical probes are given. At the lower velocities (which in practical terms are less than, say, 2 m/sec), the diffusion time is

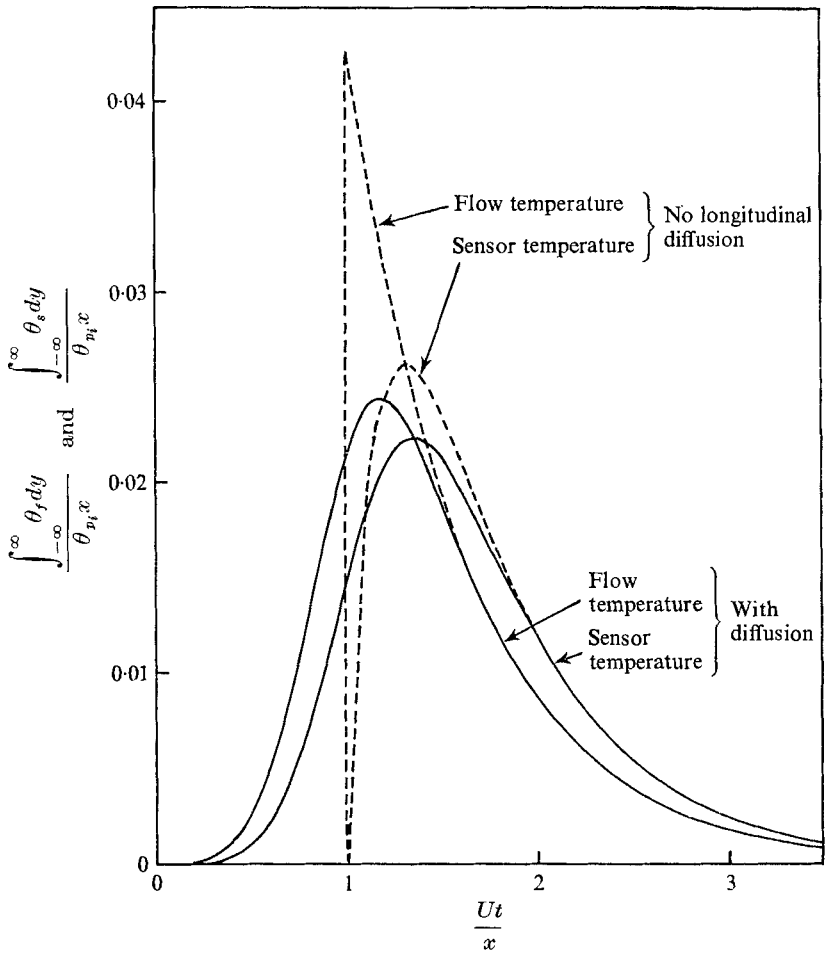

FIGURE 3. The flow and sensor-wire temperature variation, Péclet number = 30.

$$\frac{d_p}{d_s} = 2; \quad \frac{x}{d_s} = 500; \quad \frac{UT_d}{x} = 0{\cdot}730; \quad \frac{UT_s}{x} = 0{\cdot}177; \quad \frac{UT_p}{x} = 0{\cdot}600.$$

comparable to and eventually more than both the convection time and sensor-wire time constants. However, as the velocity is increased, this situation is inverted and the diffusion time rapidly becomes very short compared with the convection time and the sensor-wire time constant.

In order to typify the type of sensor-wire signals that are obtained at the two extremes of Péclet number discussed above, equations (17) and (18) have been

used to calculate both the flow temperature and sensor-wire temperature variations at two Péclet numbers of 30 and 300 for a spacing ratio, x/d_s, of 500 and a pulsed-wire to sensor-wire diameter ratio, d_p/d_s, of 2. The results, which are shown in figures 3 and 4, have a comparatively simple physical interpretation. When the diffusive front has passed (i.e. $tU/x > 1+2/P^{\frac{1}{2}}$), both the flow temperature and sensor-wire temperature approach the results obtained in which diffusion is

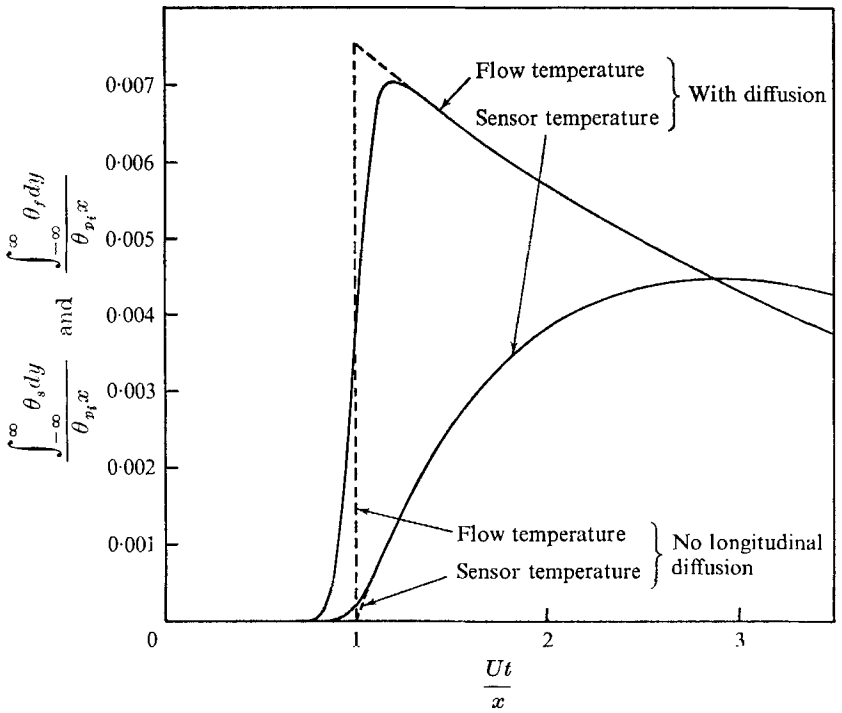

FIGURE 4. The flow and sensor-wire temperature variation, Péclet number = 300.

$$\frac{d_p}{d_s} = 2; \quad \frac{x}{d_s} = 500; \quad \frac{UT_d}{x} = 0{\cdot}231; \quad \frac{UT_s}{x} = 1{\cdot}094; \quad \frac{UT_p}{x} = 3{\cdot}595.$$

neglected, namely, equations (6) and (9). In the neighbourhood of the pulse front, the influence of longitudinal diffusion is to replace the discontinuity in slope that occurred without longitudinal diffusion by a transition region. In particular, if the sensor-wire time constant is much less than the diffusion time, the sensor-wire signal tends to follow the flow temperature variation (see figure 3). At the other extreme, when the sensor-wire time constant is much longer than the diffusion time, the relationship between the sensor-wire signal and the flow temperature given by equation (8) reduces in the neighbourhood of the diffusive front to the simple form

$$\int_{-\infty}^{\infty} \theta_s dy = \frac{1}{T_s} \int_0^t \left(\int_{-\infty}^{\infty} \theta_f dy \right) dt.$$

In other words, the sensor wire behaves initially as a simple integrator of the free-stream temperature. Under these circumstances, the transition region extends only for the duration of the diffusion time, and thereafter the signal

rapidly approaches the form given by (9) in which diffusion is neglected. It is perhaps easier to visualize these results if it is remembered that the relationship between the flow temperature and sensor-wire temperature is exactly analogous to the relationship between the input voltage applied across a resistor and a capacitor in series and the output voltage taken across the capacitor. The RC time is equivalent to the sensor-wire time constant and the results for low and high Péclet number correspond to a low and high frequency signal respectively.

The influence of diffusion is therefore to introduce some uncertainty as to precisely when the sensor-wire signal corresponds to the time of flight. A number of possibilities exist for overcoming this uncertainty but the simplest technique is that suggested by Bauer in his original paper. This involves observing the

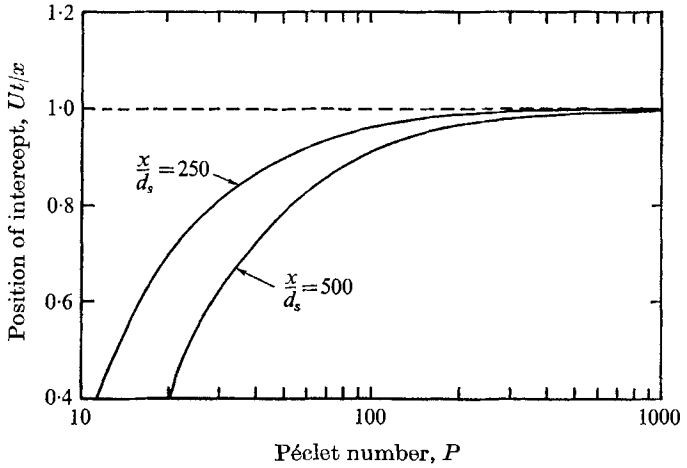

FIGURE 5. The influence of Péclet number on the intercept times. $d_p/d_s = 2$.

sensor-wire signals on an oscilloscope, and effectively extrapolating back onto the zero signal axis from the position of the maximum slope. For this to be accurate, it is necessary for the diffusion time to be small compared with the sensor-wire time constant so that the rise of the sensor-wire signal after the diffusive front has passed is still nearly linear. Figure 4 typifies such a situation. However, as the results in figures 2 and 3 show, there is always a lower bound to this technique because the diffusion time increases more rapidly than the sensor-wire time constant as the Péclet number is reduced. In order to give some idea of the errors that might be expected from this technique at the lower Péclet numbers, the position of the intercept from the maximum slope position has been calculated from equation (18) for our two typical probes. These results (figure 5) show that the intercept technique can be used down to Péclet numbers in the region of 100 without the errors being too significant. In practical terms, this corresponds to velocities of about 1 m/sec. Moreover, the experimental results discussed in § 4.2 show that the effect of the pulsed-wire viscous wake, which has so far been neglected, is to extend still further the lower bound below that suggested by these theoretical results.

Although the intercept technique has been used fairly extensively in measurements so far carried out, it is laborious in a highly turbulent flow to record a sufficient number of oscilloscope traces to determine both the mean and turbulent velocities. One alternative to the use of an oscilloscope is to digitize the signals and analyse them on a computer. This is the technique used by Tombach (1969), but it requires comprehensive facilities which were not available in the present experiments. Another possibility is to use the intercept technique with a digital counter. The counter could be set to run when the pulse is fired, and its output gated when the sensor-wire signal reached a number of predetermined trigger levels. If these trigger levels were on the near linear rise of the sensor-wire signal, the position of the intercept could be obtained from the counter readings. However, as discussed earlier, there is a strong variation in the amplitude of the sensor-wire signals with velocity so that it would be necessary to make use of a substantial number of trigger levels in order to ensure that accurate intercept positions could be obtained over a wide speed range. This technique therefore also requires sophisticated instrumentation since it is effectively equivalent to digitizing the signal except that instead of digitizing voltages at set intervals of time, one would be recording times at set intervals of voltage. In this particular problem, this is a much more efficient approach to digitization, and although a computer would still be required to analyse the signals, it is possible to envisage on-line use of the instrument using this approach whereas this is almost certainly not possible if the signal is digitized in the more usual manner.

Neither of the above techniques is very simple and a more direct approach which has been explored in the present investigations is to make use of the differentiated sensor-wire signals. In the absence of diffusion these differentiated signals would exhibit a sharp step at $tU/x = 1$, and a counter could be triggered at any level below the step amplitude to obtain the time of flight. The variation in the step amplitude in the absence of diffusion is given by (10), and, as has already been discussed, this exhibits a much slower variation with free-stream velocity than the amplitude of the undifferentiated signal. The effect of diffusion is again to smooth out the step discontinuity, and figure 6 shows typical results obtained by differentiating (18) and calculating the output signals for a probe with $x/d_s = 500$ and $d_p/d_s = 2$. For a trigger level fixed at a signal level corresponding to

$$(x^2/\kappa)\, d\left[\int_{-\infty}^{\infty} \theta_s dy \Big/ (\theta_{p_i} x)\right] \Big/ dt = 1,$$

the time of flight obtained in this way is shown in figure 7 as curve 1. These results show that if a departure from linearity of, say, 5 % on velocity is regarded as acceptable then this technique could be used down to Péclet numbers in the region of 100 again. The advantage of this technique is that it is not too sensitive to the trigger level setting. For example, if the trigger level were set at a signal level corresponding to

$$(x^2/\kappa)\, d\left[\int_{-\infty}^{\infty} \theta_s dy \Big/ (\theta_{p_i} x)\right] \Big/ dt = \frac{1}{2},$$

the time of flights results would now be as shown in curve 2 in figure 7. Although these latter flight times are below the true flight times, the calibration would still

be reasonably linear over a Péclet number range from 150 to 1000, and in any case, the influence of the slight non-linearity in the calibrations could be removed in the subsequent computation of the results.

With this description of the sensor-wire signals in steady flow, the experimental problems of using a pulsed-wire probe can now be discussed.

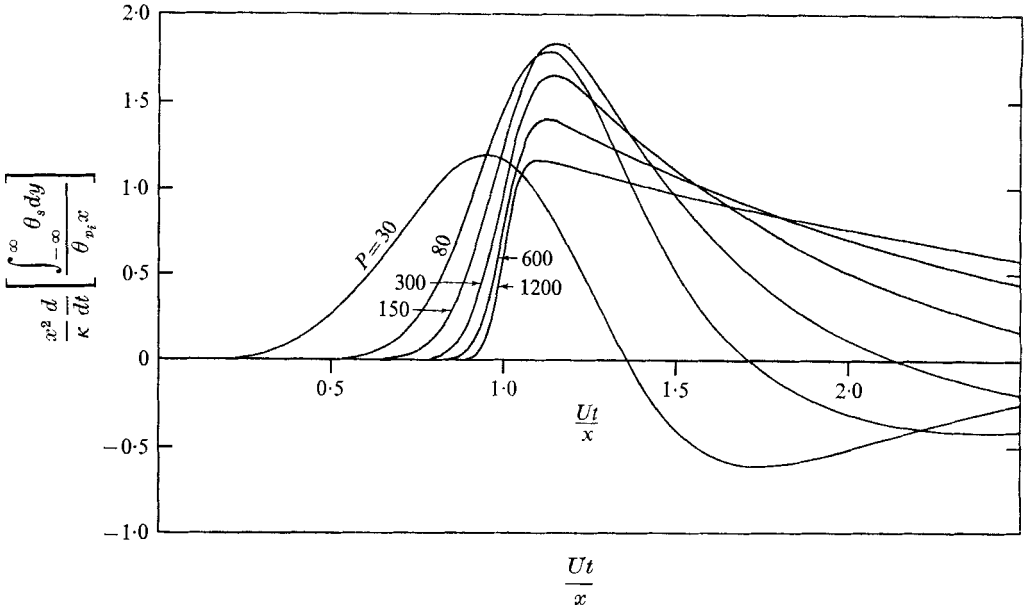

FIGURE 6. Examples of differentiated sensor-wire signals at different Péclet numbers. $x/d_s = 500$; $d_p/d_s = 2$.

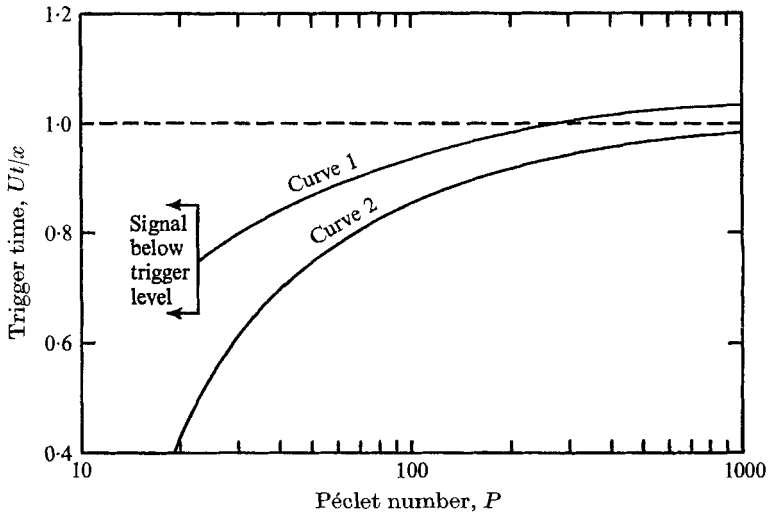

FIGURE 7. The influence of Péclet number and trigger level on the differentiated signal trigger times. $d_p/d_s = 2$.

3. Details of the experiments

The design of pulsed-wire probes and the way in which they are operated depends not only on the dynamics of the convection and diffusion of the heat pulse but also on some of the practical electronic and mechanical constraints that arise. These include problems of signal-to-noise ratio and the influence of electrical coupling between the pulsed-wire and sensor-wire circuits. As these factors are of central importance to the successful development of the technique, they will be discussed in some detail.

3.1. *The probe design and its electrical circuitry*

All the probes used have been broadly similar to the one sketched in figure 1. Most of the experiments have been carried out with sensor wires of $5\,\mu$ diameter platinum and with pulsed wires of either $10\,\mu$ diameter platinum or $10\,\mu$ diameter nickel wire. Both platinum and nickel are suitable materials for pulsed wires

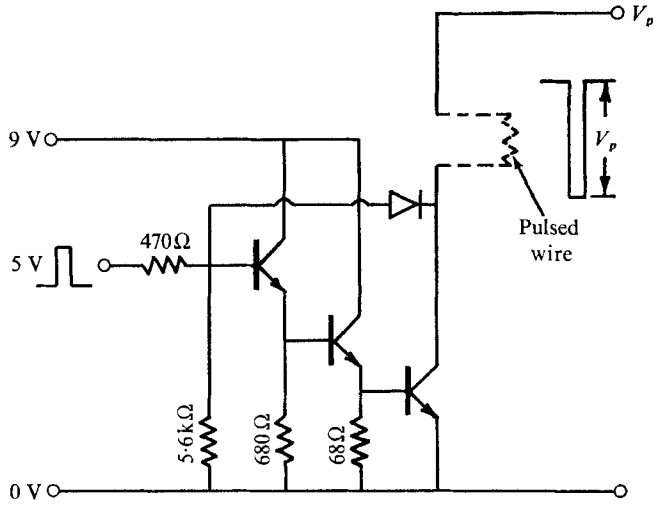

FIGURE 8. The transistor switch (Texas 2M2243 transistors).

because they are capable of operating at high temperatures (i.e. in excess of 600 °C) without oxidizing. On the other hand, tungsten wire, which is admirably suited for use as the sensor wires, is not suitable for pulsed wires because it oxidizes at the comparatively low temperature of about 300 °C.

The duration of the pulses used to produce the tracer of heated air ranges from a few microseconds up to about $30\,\mu$sec with peak currents as high as 8 amps although a more typical figure is 4 amps. Although there is nothing intrinsically difficult about making a circuit to produce such pulses, figure 8 shows the circuit for the transistor switch used in the present experiments. A number of types of transistor were tried, but those shown are particularly satisfactory in giving pulses with a rise and fall time of better than $0{\cdot}5\,\mu$sec. The circuit can switch a current of about 4 amps through any resistance with a limitation on the transistor of a maximum collector voltage V_p of about 80 volts. For higher currents, two of

the switches can be operated in parallel. The switches give pulses of almost constant voltage and they can be driven from an ordinary low power pulse generator.

The sensor-wire circuit that is of interest for the moment is only the simple bridge and low-noise amplifier part of the circuit shown in figure 9. The rest of the circuit relates to the automatic aquisition of the times of flight and will be discussed later in § 6. The two sensor wires are operated as arms in a simple bridge with the current supplied by an ordinary 1·5 volt dry cell battery. The output is taken across the bridge centre points so that the polarity of the signal depends on which sensor wire picks up the heat pulse; the signal polarity therefore gives the flow direction. The only major problem with the sensor-wire circuit arises from the electrical coupling between the pulsed-wire circuit and sensor-wire circuit. Although these two circuits are not connected by any 'real' wires, there is in reality both capacitative and inductive coupling between the two circuits, especially at the probe head where the wires and their supports form parallel loops admirably designed to maximize mutual inductance! In principle, operating the wires in the arms of a bridge should cancel out any common-mode interference signal but, for a variety of reasons, this does not occur and, every time a pulse is fired, there is a pick-up signal on the sensor-wire circuit of a few millivolts – this is many times larger than the sensor-wire signal from the heat tracer which is typically about 100 μV. This pick-up signal is of a short duration and, in itself, is not important. But, if any low-pass filtering is used to improve the signal-to-noise ratio, the interference signal acquires a decay time which is of the order of the reciprocal of the cut-off frequency. This causes difficulties at higher speeds as will be discussed later.

We turn now to the design of the probe itself and the influence of signal-to-noise ratio considerations both on the geometry of the probe and the operating current through the sensor wires. If an extensive yaw response of, say, $\pm 70°$ is required, it is necessary that all the probe wires should be about five times longer than the spacing between the pulsed wire and the adjacent sensor wires. As far as the influence of signal-to-noise ratio is concerned, two factors should be noted. First, provided the sensor wire is long enough to intercept the entire heat pulse, the sensor-wire signal is independent of the wire length. Second, as discussed in § 2.3, we would expect from heat conservation arguments that the amplitude is not dependent on the spacing between the pulsed wire and sensor wires apart from the usually weak influence of longitudinal diffusion and possibly also the effect of the pulsed-wire viscous wake. We have therefore the somewhat surprising situation that neither the spacing nor the wire length have a very strong influence on the signal amplitude. On the other hand, noise will be directly proportional to the wire length; this includes both electronic noise from the amplifier and also any response that the sensor wire has directly to the airstream flowing past it either to temperature fluctuations as a resistance thermometer or to velocity fluctuations as a hot-wire anemometer; these sources of noise will be discussed shortly. It would appear therefore that there is a strong motive to reduce the spacing between the wires as much as possible, and this would also be helpful in reducing the size of the probe relative to the length scales of the

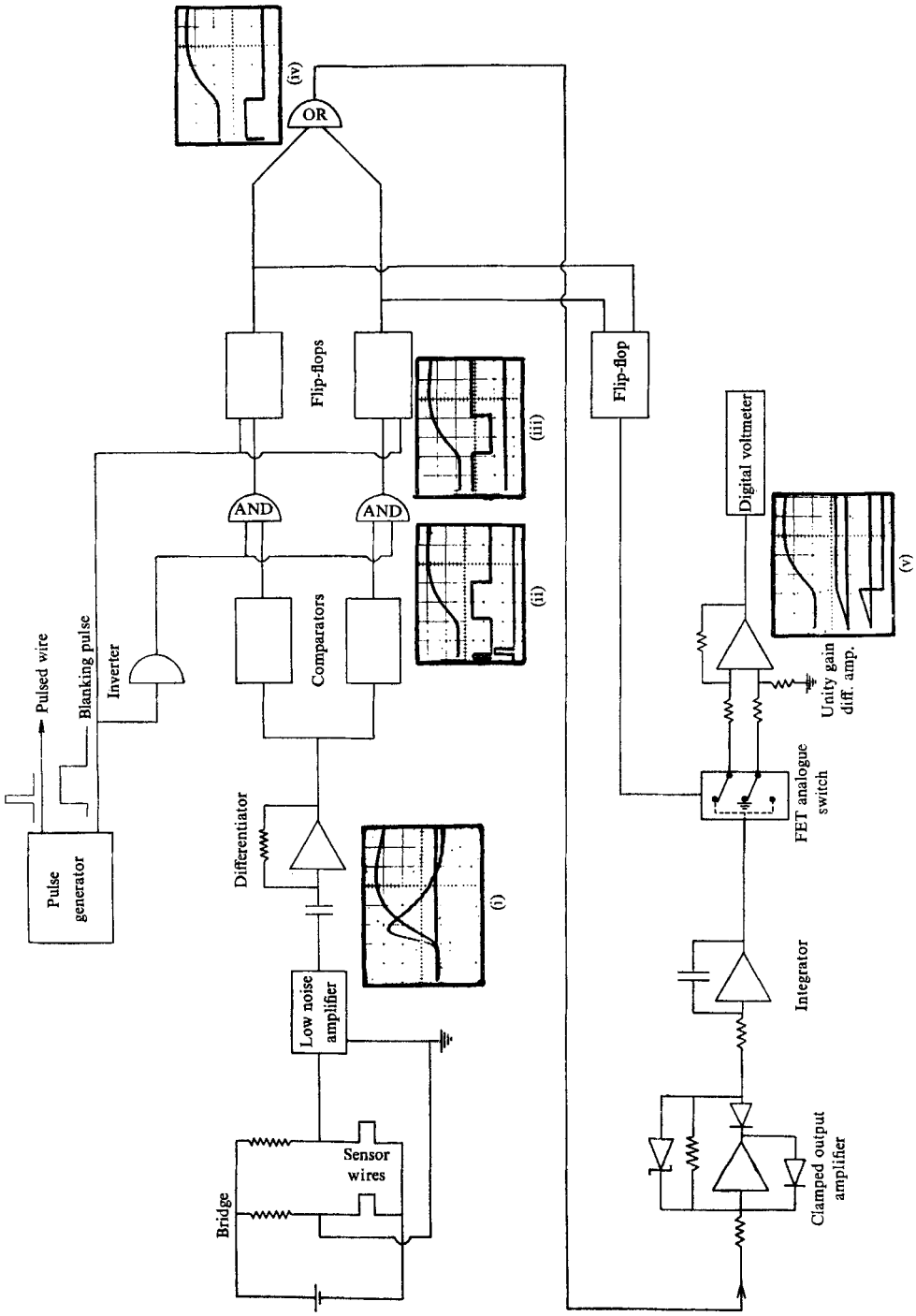

FIGURE 9. Circuit for the automatic measurement of flight times.

turbulence. However, there are two factors which set a broad limit to the permissible reduction of this spacing. The first is that it does not seem advisable to reduce the Péclet number below, say, 50 even though the experimental results discussed later in § 5 show that the influence of longitudinal diffusion on the apparent time of flight is much less than might be expected from the theoretical arguments in § 2.4. If we set 1 m/sec as a typical lower bound on velocities of interest, this gives a spacing of about 1·25 mm for a Péclet number of 50. On the other hand, at the higher velocities, the time of flight eventually becomes comparable to the decay time of the pick-up signal discussed earlier, and the signal from the heat pulse merges into the decaying 'tail' of the interference signal. This decay time is typically 100 μsec which therefore limits the maximum speed for a 1·25 mm spacing to about 14 m/sec. Thus, from a consideration of these various factors, it would seem that, with the present experimental arrangements, it is expedient for the spacing between the pulsed wire and sensor wires to be not less than about 1·25 mm. In order to obtain an adequate yaw response, this requires that the wire lengths should not be less than about 6·25 mm say. This is a much larger probe than the average hot-wire anemometer, and it might seem that errors due to the probe size might be more significant than in the case of a hot-wire anemometer. However, as will be discussed later in § 5, experiments so far carried out do not show any strong effects under normal conditions, and it is certainly possible to carry out investigations in the normal wind-tunnel environment although the larger scale of flow encountered, say, in meteorology and in heating and ventilating problems would provide an admirable area in which to apply the technique.

We also have to consider the problem of choosing the sensor-wire current for the optimum signal-to-noise ratio. In addition to the electronic noise from the amplifier, the wire appears to retain some sensitivity to the airstream flowing past it. At very low currents (say, below 1 milliamp for a wire of 5 μ diameter), this is probably due to small temperature fluctuations that occur in the stream but, as the current is increased (say, above 5 milliamps), the wire begins to respond like an ordinary hot-wire anemometer to fluctuations in the velocity. No attempt to examine this problem quantitatively has yet been made but it seems likely that the 'noise' output will be of the form

e	$+$	$a_1 i$	$+$	$a_2 i^2$
Electronic noise from amplifier		Response to temperature fluctuations in the stream		Response to velocity fluctuations in the stream

where a_1 and a_2 depend not only on properties of the wire, but also on the magnitude of the velocity and temperature fluctuations that occur in the stream. The signal level will tend to vary directly with the current so that the signal-to-noise ratio behaves like $i/(e + a_1 i + a_2 i^2)$. Initially, this ratio increases with current; it then reaches a maximum and, finally, when the wire begins to behave substantially like a hot-wire anemometer, the signal-to-noise ratio will fall away like $1/i$. This seems to accord with one's impressions when carrying out experiments, and it is a fairly simple matter to adjust the current to obtain a reasonable signal-to-noise ratio. For 5 μ diameter platinum sensor wires, this current invariably lies in the region of between 0·5 and 3 milliamps. Below 0·5 milliamps, the

influence of electronic noise begins to be significant whereas if the current exceeds 5 milliamps, say, the wire clearly begins to respond directly to velocity fluctuations.

One final point about the probe design should be made. The thermal stresses set up when the pulsed wire is heated can cause it to mechanically vibrate the rest of the probe. The resulting strain gauging of the sensor wires gives a spurious signal which partially obscures the convected heat pulse signal. This problem can be overcome by ensuring that the pulsed wire is not taut across the probe supports. In cases where mechanical 'ringing' occurs, it is invariably sufficient to kink the pulsed wire carefully to eliminate the problem.

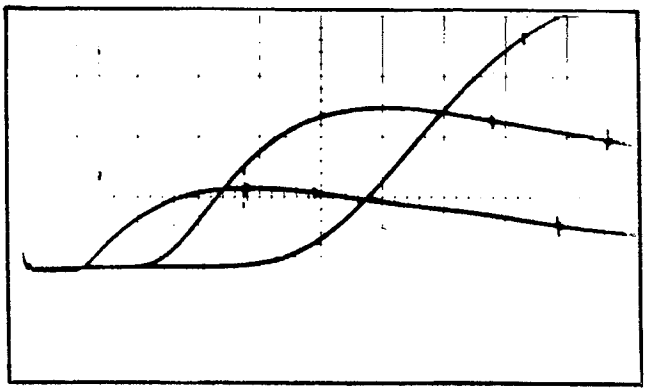

(*a*)

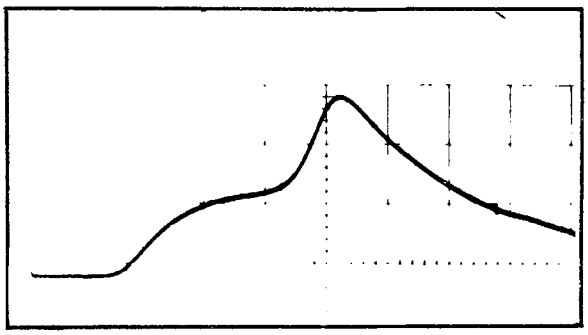

(*b*)

FIGURE 10. Examples of sensor-wire signals. (*a*) At different flow velocities, sweep speed 0·5 msec/cm. (*b*) In turbulent flow.

4. Results of calibration experiments

Some typical signals for a crossed-wire probe in steady flow are shown in figure 10(*a*). They exhibit all the features discussed earlier and a number of careful calibrations have been carried out to compare with the theoretical results. The aim of this work was to try to highlight any problem areas in obtaining a proper understanding of the pulsed-wire probe behaviour. It is worth pointing out at the outset that it is not easy to make these comparisons with any accuracy because, in addition to the basic observations of the sensor-wire signals, it is

necessary to know a good deal about the experimental environment. For example, it is necessary to know the lengths and diameters of both the pulsed and sensor wires, the correct heat-transfer relationship from the wires to the airstream, the pulsed-wire temperature, the temperature coefficient of the wire material and the resistance per unit length of the sensor wires and current passing through them. Some of these quantities are easy to obtain and others are not so easy, but the combination of them all and the need during the calibration experiment itself to avoid breaking any of the wires, all result in an experiment which is difficult to keep under proper control.

4.1. *The pulsed-wire temperature*

In order to make comparisons with the theoretical results, it is necessary for the pulsed-wire temperature at the end of the pulse, θ_{p_t}, to be known. Equation (3) gives this in terms of the voltage per unit length and duration of the pulse. It should be noted that the wire diameter does not enter into the relationship in this form. Before carrying out the calibration experiments, it seemed a prudent exercise to check whether the temperatures given by this expression were achieved in practice. A number of different diameter wires were used with pulse lengths ranging from $5\,\mu$sec to $35\,\mu$sec. The voltage and current applied to the wire were obtained from oscilloscope traces similar to the one shown as an inset in figure 11. The current trace was obtained using a Tetronix current probe. The temperature rise at the end of the pulse was obtained from the observed resistance change. The experimental values obtained in this way are compared with the equation (3) in figure 11, and the agreement is reasonably satisfactory. The values of the first temperature coefficient of resistance, α, and the resistivity, σ, used in evaluating the results are 0·0035/°C and 11·2 ohm cm both based on 0 °C. These differ slightly from the values for pure platinum and they were obtained from the experiments of the present authors on the heat-transfer laws for fine wires. In the absence of any better guide, the other properties of the wire material were assumed to be the same as for pure platinum. Although no great claim is made for the accuracy of the experiments, the experimental results do lie consistently below the values obtained from equation (3). This discrepancy is not greatly affected by the values of the material properties used, and it would appear to be a genuine discrepancy. It cannot, however, be attributed to heat conduction, convection, or radiation losses, because these would have shown up as a variation in the experimental results for different duration pulses. No satisfactory explanation can be offered for the discrepancy at the moment, but, since some electrical 'ringing' was apparent in the voltage pulse, it may be simply due to the capacitance or inductance of the pulsed-wire probe and the leads to it.

It is also worth pointing out that the lifetime of a pulsed wire is strongly dependent on the temperature to which it is pulsed. For platinum, it would appear that, provided this temperature does not exceed about 500 °C or 600 °C, the lifetime of the wire is virtually indefinite. However, once the temperature is taken above this point, the lifetime becomes extremely uncertain. In some cases, a wire can be operated for long periods at pulsed temperatures in the region of 1000 °C, but, on other occasions, the wire will break after one or two pulses. Since

it is an advantage from the point of view of a good signal-to-noise ratio to always operate the pulsed wire at as high a temperature as possible, there is a continual temptation to operate at the very elevated temperatures with the result that one becomes very adept at replacing wires. In the calibration experiments, the wires were deliberately operated at a very conservative temperature in order to minimize the possibility of breaking the pulsed wire before the experiments were completed. It is also worth noting that every time a wire is pulsed, it produces an audible 'click', and this provides a quick check on whether or not the pulsed wire and its associated circuitry is operating correctly.

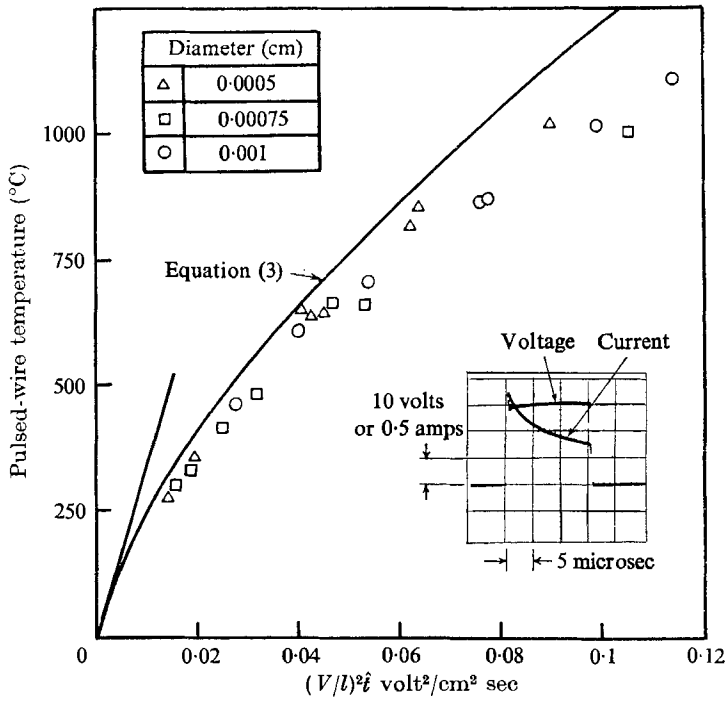

FIGURE 11. Pulsed-wire temperature. Insert is a typical voltage and current pulse.

For the purpose of comparison with the theoretical results of sensor-wire signals, the pulsed-wire temperatures have been taken as the mean of the experimental values and the values obtained from equation (3). In this way, the pulsed-wire temperatures should not be in error by more than about 10 %.

4.2. *Steady velocity calibrations*

From oscilloscope traces of the sort shown in figure 10(*a*), comparisons with the theoretical results obtained earlier are possible. To simplify the comparisons, only measurements of the intercept time, the maximum amplitude and the time to the maximum amplitude have been obtained from the trace photographs. These quantities can conveniently be used to give an indication of the agreement between the theoretical and experimental results. In addition, a calibration was carried out at very low velocities (down to 0·3 m/sec), and these traces were digitized on a Northern Instruments Memory Oscilloscope.

The mean-flow calibrations obtained from the position of the intercepts are shown in figure 12 for two probes, and they are typical of the many calibrations that have been obtained. In both cases, it was difficult to obtain accurate time-of-flight measurements at the highest velocities shown because of the electrical pick-up signal. The calibration shown for probe A was particularly carefully carried out, and included the digitized results at very low velocities. The apparent spacing between the pulsed and sensor wires obtained from the calibration was 1·68 mm for probe A and 2·92 mm for probe B. These appear to be about 10 % greater than the measured spacings which is presumably some measure of the general influence of the pulsed-wire viscous wake.

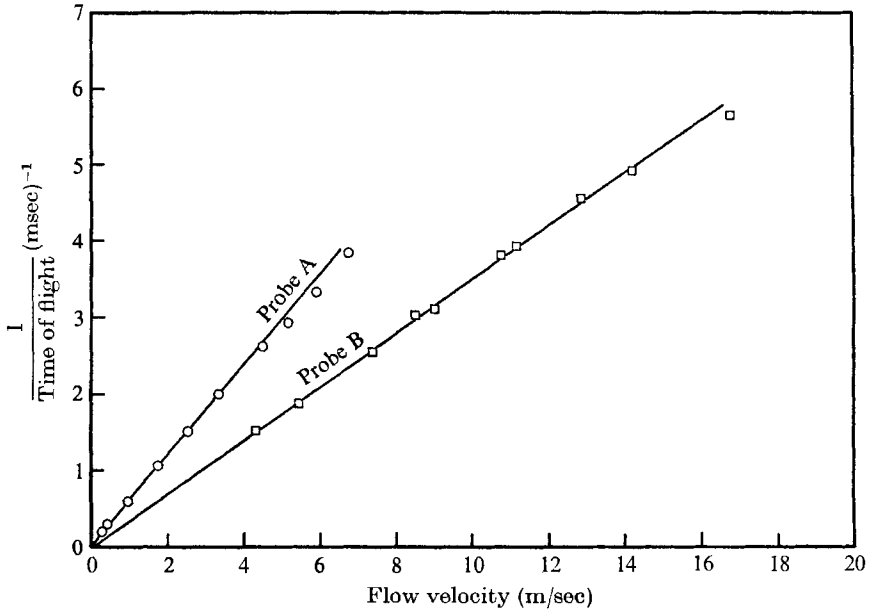

FIGURE 12. Crossed-wire probe calibrations from intercept times.

The theoretical variation of the maximum signal and the time to this maximum signal are shown in figures 13 and 14 respectively where they compared with the experimental results. The agreement is quite satisfactory in showing the general trends although, as has already been explained, very precise agreement cannot perhaps be expected. The influence of longitudinal diffusion on these results is very small, and the results differ significantly from the simple expressions given as equations (11) and (12) only for Péclet numbers below about 40.

Finally, figure 15 compares the complete digitized signals obtained at low velocities with the theoretical distributions. These comparisons are very interesting because they seem to show a clear influence of the pulsed-wire viscous wake on the time of flight. At the highest velocity shown (1·73 m/sec and a Péclet number of 140), the agreement between the theoretical and experimental signal is very good, and the signal is typical of those in which the effects of thermal diffusion are small (cf. figure 4). However, the theoretical distributions at the two lower velocities (0·98 m/sec and 0·28 m/sec, corresponding to Péclet numbers of

80 and 23 respectively) show that thermal diffusion has moved the intercept positions well forward of the convective time of flight $tU/x = 1$ as has already been illustrated in figure 5. But, the experimental results do not exhibit this same

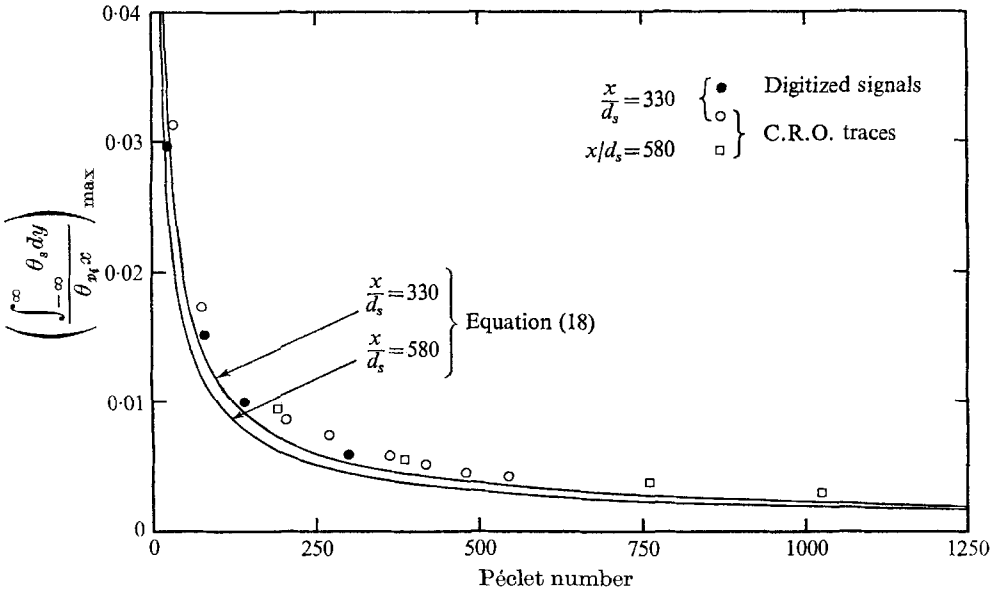

FIGURE 13. Amplitude of sensor-wire signals.

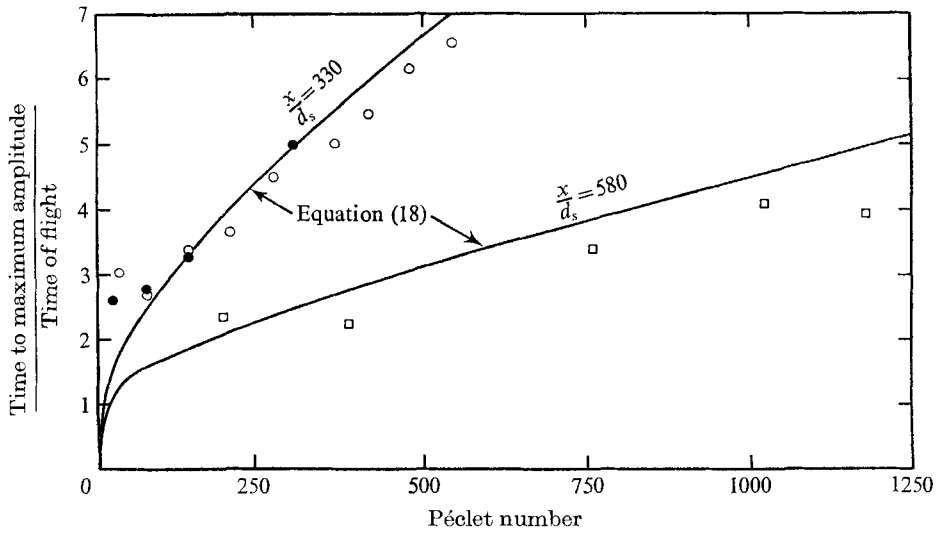

FIGURE 14. Time of maximum amplitude of sensor-wire signals. See figure 13 for symbols.

forward movement of the intercept position, although the shapes of the signals are very similar to the theoretical distributions. This is probably due to the increasing influence of the viscous wake at low Reynolds numbers, and it would appear fortuitous that probe calibrations remain linear at Péclet numbers well

below those at which thermal diffusions effects might have been expected to have a strong influence on the apparent time of flight. Although this appears to be generally true, it is obviously an area where more work is required.

4.3. *Yaw response*

Although it would be possible to calculate a theoretical yaw response from the work in § 2.4, it is sufficient for present purposes to discuss the response in more general terms.

The yaw response of a pulsed-wire probe has to be considered in two planes at right angles to one another. Consider first the situation in which the direction of

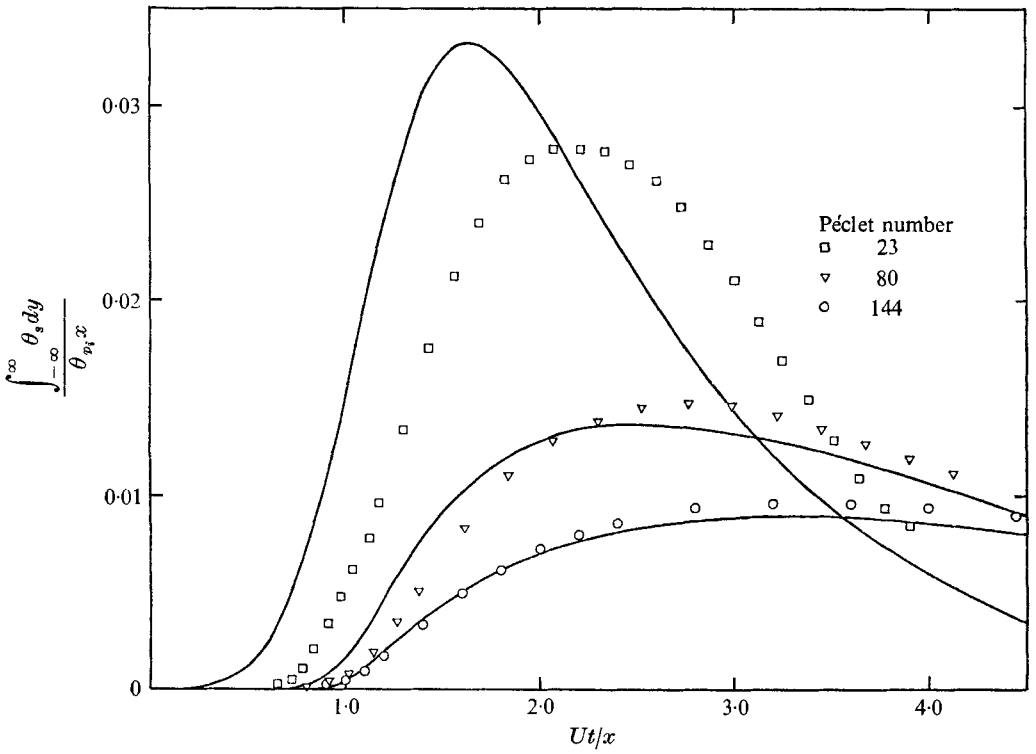

FIGURE 15. Comparison between theoretical and experimental sensor-wire signals. $d_p/d_s = 2{\cdot}1$; $x/ds = 330$. ——, equation (18).

lateral diffusion is along the axes of the sensor wires. If we assume that only the normal component of velocity is effective in the heat transfer to and from wires, the only influence of the yaw is to decrease the effective Péclet number by a factor $(\cos\theta)$ compared to the unyawed case. Consequently, the yaw response should be close to the ideal cosine response for the higher Péclet numbers, and the results shown in figure 16 would seem to confirm that this is the case. As far as the signal amplitudes are concerned, these will increase with yaw because of the reduction in the effective Péclet number (see equation (11)) and the variation will lie between $1/\cos\theta$ and $1/(\cos\theta)^{0{\cdot}55}$ depending on the pulsed-wire Reynolds number.

The results in figure 16 are not inconsistent with this argument. At the very large yaw angles, the influence of the wire supports begins to manifest itself, and the signal amplitudes decrease. Also there is some variation in the time of flight due to the wake from the probe supports, but a useful response is nevertheless maintained up to angles in the region of 80°.

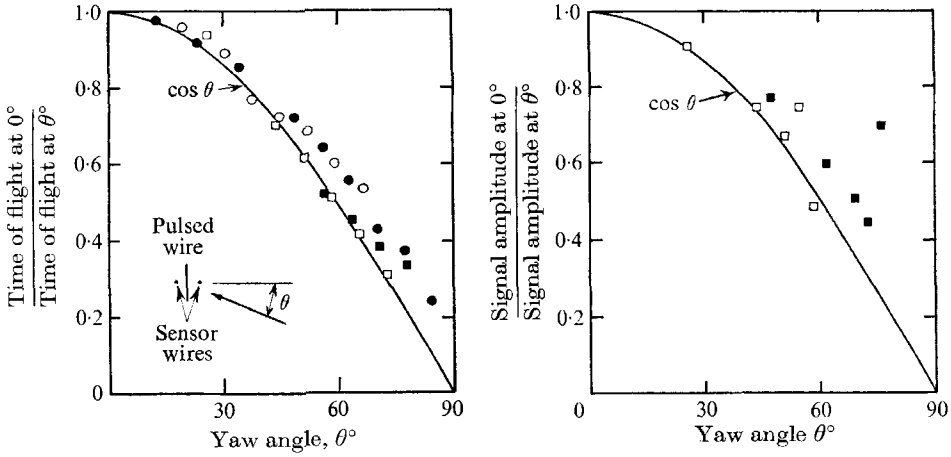

FIGURE 16. Yaw response of crossed-wire probe. Closed and open symbols refer to opposite sides of the axis of symmetry. ○, ●, 1·7 m/sec; □, ■, 7·4 m/sec.

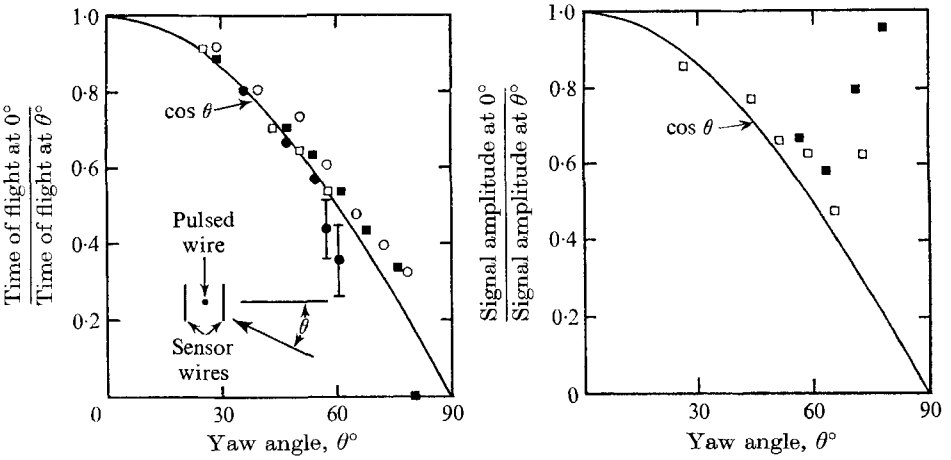

FIGURE 17. Yaw response of crossed-wire probe. See figure 16 for symbols.

When the probe is yawed in the other plane, lateral diffusion spreads the pulse in the plane at right angles to the sensor-wire axes, and it has the effect of increasing the duration of the diffusive front of the pulse by a factor $1/(\cos\theta)$ for small angles of yaw. However, for the higher Péclet numbers, the position of the intercept should not be significantly affected by the yaw, and the results in figure 17 again show this to be so. Because the sensor wires are now cutting across the width of the pulse, one would expect the signal amplitudes to increase with yaw angle initially like $1/(\cos\theta)$ although there will also be a weak influence from variations in the sensor-wire time constant due to the yaw. The results in figure 17

show that the amplitudes do increase in roughly this way although, at very large yaw angles, the amplitudes again diminish due to probe interference.

5. Measurements in a turbulent flow

Having established the general behaviour of the probe, its application to turbulent flow measurements can now be considered. There are two techniques for turbulent flow measurements which have so far been used. The first and simplest is to display the sensor-wire signals on a storage oscilloscope and estimate the intercept positions from these traces. Although this is laborious, it is quite feasible to make measurements in this way provided that not too many measurements need to be made. The measurements behind bluff bodies of Bradbury (1969) and Castro (1971) were made in this way. However, if extensive measurements are to be made, an automatic means of recording the flight times is needed and a system is described in § 6 which has now been used in a variety of highly turbulent flows. However, whatever system of recording flight times is used, it is necessary to consider the influence of the turbulence on the probe response.

The first point is to have some guide as to the number of flight times that it is necessary to record in order to achieve a prescribed accuracy. For normally distributed velocity fluctuations, the appropriate approximate expressions for the estimation of sample size in the determination of the mean velocity and intensity are (Mandel 1964)

$$n = \frac{t^2\overline{u^2}}{(\Delta U)^2}; \quad n = \frac{t^2\overline{u^2}}{2(\Delta(\overline{u^2})^{\frac{1}{2}})^2}, \tag{19}$$

where n is the number of samples taken in order to ensure that estimates of the mean velocity and turbulent intensity are within $\pm\Delta U$ and $\pm(\Delta(\overline{u^2})^{\frac{1}{2}})$ respectively of the true values. t is a parameter called the Student's t-distribution function which has values of 1·96 for a 95 % probability of being within the interval and 1·645 for a 90 % probability. These are approximate expressions and they assume that the number of samples taken is large which, in this case, means greater than, say 50. As an example, if the turbulent intensity relative to some reference velocity was 50 %, then, in order to determine the mean velocity to within ± 5 % of the reference velocity with 95 % probability, it would be necessary to record 385 flight times. Under these circumstances, the intensity would be within 6·9 % of the true intensity with 95 % probability. These estimates do not, of course, include the effects of experimental errors.

We turn now to a discussion of the reduction of the time-of-flight measurements. The most satisfactory way of reducing the data is to plot the integrated velocity probability distribution. This involves simply plotting the number of signals n that are present in the velocity range from $-\infty$ to u_n, say. Figure 18 shows such a distribution obtained in a reverse flow region using intercept measurements from a storage oscilloscope. The mean velocity U is given by

$$U = (1/N)\int_0^N u_n\,dn,$$

where N is the total numbers of sample taken. It is worth mentioning that, when an oscilloscope is used, there is inevitably a velocity range in these distributions centred about the zero velocity point for which tracer signals will not appear on the oscilloscope screen at all; this band is shown in figure 18 for the particular sweep speed used. As a consequence, the shape of the probability distribution in this range cannot be determined. However, provided these 'no signal' traces are counted in the results, the probability distributions should still be correct outside this region and a smooth curve can usually be drawn through the experimental points. In fact, the act of drawing a 'smooth' curve through a limited

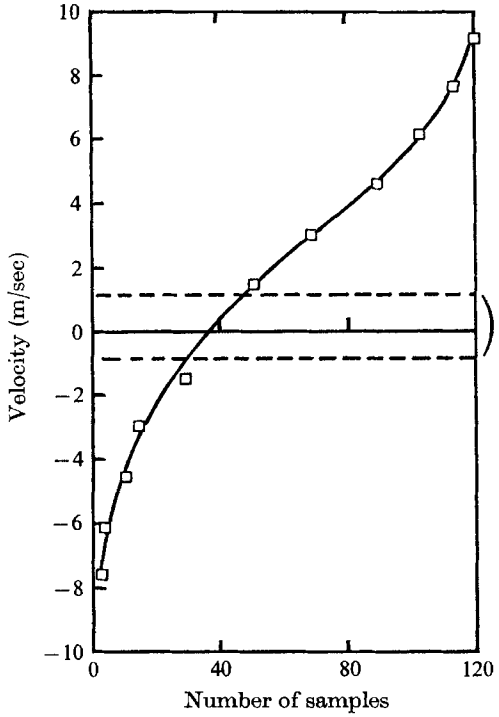

FIGURE 18. Integrated probability distribution in the region one diameter downstream from a circular cylinder. Region in between dotted lines is velocity band not observable on the oscilloscope.

number of experimental points on the probability curve almost certainly gives a higher accuracy for the estimation of the mean velocity and intensity than would be expected from the straightforward statistical expressions given earlier (equations (19)). Another source of error is that, even with an automatic means of recording flight times, some heat tracers will miss the sensor wires in a highly turbulent flow because of the finite yaw response of the pulsed-wire probe. The errors arising from these missed tracers will be considered in a moment, but it is again important from accuracy considerations to include these as zero-velocity results as should the occasional ambiguous signals which occur. These latter signals result presumably from heat pulses arriving at the limit of the probe yaw response.

Having obtained the mean velocity, the probability distribution can also be used to determine the turbulent intensity since

$$\overline{u^2} = (1/N)\int_0^N (u_n - U)^2 dn.$$

Intensity estimates from storage oscilloscope measurements are certainly less accurate than the mean velocity results because large deviations from the mean velocity contribute strongly to the intensity level, and these are precisely the readings which are difficult to obtain accurately on an oscilloscope. The very high velocities require the measurement of a small distance on an oscilloscope and the very low velocity signals may not appear on the screen at all! Automatic methods of recording flight times, however, considerably reduce experimental errors of this sort.

We consider now errors arising from the tracers which the sensor wires do not pick up because of the finite yaw response of the pulsed-wire probe. In order to give some idea of the errors, the case of a normally distributed isotropic turbulent flow has been considered for which it is possible to obtain some surprisingly simple expressions (see appendix). If the probe is capable of picking up heat-tracer signals within two cones of half angle ϕ, one on either side of the pulsed wire, then the probability of missing a heat tracer is

$$p = \cos\phi \exp\left[\frac{-\sin^2\phi}{2(\overline{u^2}/U^2)}\right]. \tag{20}$$

It should be noted that as $\overline{u^2}/U^2 \to \infty$, then $p \to \cos\phi$ which, as one would expect, is simply the ratio of the area of the sphere subtended externally to the two cones to the total area of the sphere. The error arising from the missed 'tracers' in the case of the mean velocity is

$$\frac{E(U)}{U} = \frac{U_m - U}{U} = -p\cos^2\phi, \tag{21}$$

where U_m is the estimated mean velocity and U is the true mean velocity. In the case of the intensity, the error is

$$\frac{E((\overline{u^2})^{\frac{1}{2}})}{(\overline{u^2})^{\frac{1}{2}}} = \frac{((\overline{u^2})^{\frac{1}{2}})_m - (\overline{u^2})^{\frac{1}{2}}}{(\overline{u^2})^{\frac{1}{2}}} = \left[(1 - p\cos^2\phi) + \frac{p\cos^2\phi}{\overline{u^2}/U^2}[2 - \cos^2\phi(1+P)]\right]^{\frac{1}{2}} - 1. \tag{22}$$

In both cases, the 'missed' tracers are included in the estimates as zero-velocity results. For the sake of brevity, it is perhaps appropriate not to devote too much time to an analysis of these results since this can be left to the interested reader. However, as an example, figures 20 and 21 show the relative errors in mean velocity and intensity as a function of the turbulent intensity for probes with yaw limits of 50°, 60° and 70°. As far as mean velocity is concerned, the significance of these results needs to be considered fairly carefully in order to avoid obtaining an incorrect impression of the errors. For example, as the intensity tends to infinity, the relative error in mean velocity tends to $(-\cos^3\phi)$. However, the limit of infinite intensity corresponds in practice only to a turbulent free

stagnation point so that a finite relative error in the measurement of a zero mean velocity may not be too important! In many cases, it is more appropriate to relate the errors to some fixed reference velocity such as the free-stream velocity and, for the majority of experiments, even the 50° probe would give acceptable

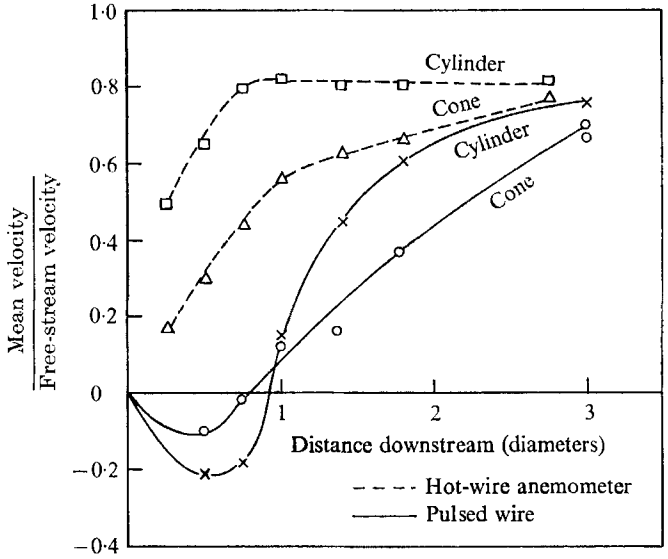

FIGURE 19. Pulsed-wire and hot-wire anemometer measurements of mean velocity behind a cylinder and a cone.

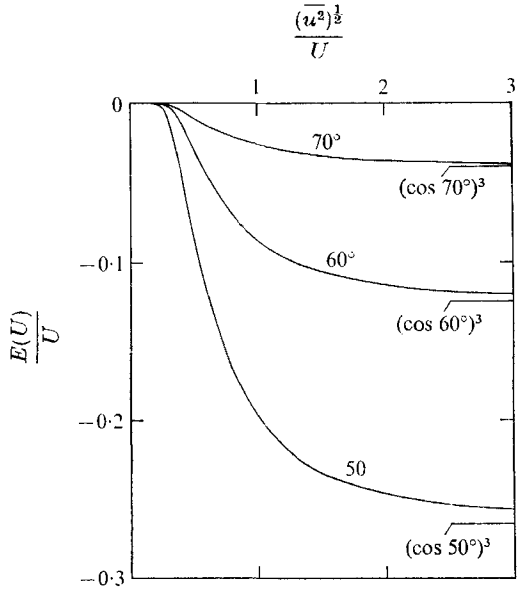

FIGURE 20. The error in the measurement of mean velocity due to the probe finite yaw response.

results for the measurement of mean velocity. The results for intensity are more intriguing. As the intensity tends to infinity, the relative error in the intensity tends to $-([1-\cos^3\phi]^{\frac{1}{2}}-1)$. Again, a probe with a yaw limit of 50° would be

acceptable for many experiments at these high turbulence levels. But, the intensity error also exhibits a maximum at a much lower intensity. This arises from the $(p\cos^2\phi)/(\overline{u^2}/U^2)$ term in equation (22) which has a maximum when $(\overline{u^2})^{\frac{1}{2}}/U = \sin\phi/2^{\frac{1}{2}}$ and, in fact, the maximum intensity error occurs very close to this intensity. The reason for this error must be that when the root-mean-square angle of the fluctuations is close to the yaw limit of the probe, the 'missed' tracers make a strong and erroneous contribution to the intensity measurement whereas, at the higher intensities, the probability of genuine zero-velocity signals occurring

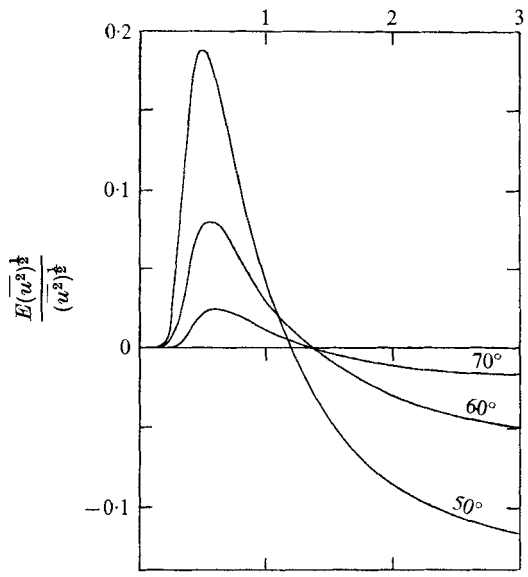

FIGURE 21. The error in the measurement of turbulent intensity due to the finite yaw response of the probe.

is higher, and the influence of the missed tracers is not then so significant. It would appear that if measurements over an extensive range of intensities are to be made, it is necessary to have a yaw limit of not less than, say, 60° if errors of 10 % or more are to be avoided.

In the discussion so far, the effect of the probe size relative to the length scales of the turbulence has been neglected. It has proved extremely difficult to make any analytic estimates of the effects of finite probe size but the following general comments may be of interest. There seem to be two main effects. The first concerns the effect of the probe size on the accuracy of the measurements. If we neglect for the moment the influence of longitudinal diffusion, the sensor wire of a large probe in turbulence would still exhibit a discontinuity of slope when the pulse front arrived. However, this time of flight would correspond to the most rapidly arriving part of the pulse front and it is not difficult to see that this would give rise to values of the mean velocity that were too large and values of intensity that were too small. The length of a sensor wire in a probe which intercepts signals

is of the order of $x((\overline{v^2})^{\frac{1}{2}}/U)$ where x is the spacing between the pulsed and sensor wires, and $((\overline{v^2})^{\frac{1}{2}}/U)$ is the ratio of the turbulent intensity along the wire axes to the local mean velocity normal to the probe. We might expect the error in the measurements to be a function of this length to some characteristic length scale of the energy bearing eddies, say, the integral scale, L_x. Attempts to estimate this error analytically have not yet proved successful, but a single experiment has been carried out in a turbulent stream with a turbulent intensity of about 45 %. In this experiment, measurements of both mean velocity and intensity were made with different spacings between the pulsed and sensor wires corresponding to a range from $0{\cdot}4L_x$ to $2{\cdot}0L_x$. No consistent variation in the mean velocity and intensity estimates with different spacings was found and, in fact, surprisingly good agreement with hot-wire anemometer measurements was obtained within the confidence limit of the sample size taken, in this case ± 4 % of the local mean velocity. It would appear therefore that probe size effects may be generally less significant than one might expect from a probe which has wire lengths typically two or three times those of an ordinary hot-wire anemometer probe. The other point to be considered on probe-size effects is the influence of the small-scale turbulence on the probe response. As a means of illustrating this problem it is useful to refer to figure 10(*b*) which shows a sensor-wire signal that is typical of those obtained in the present experiments in turbulent flows. There is little ambiguity about the arrival of the pulse front, but subsequently, the signal becomes irregular due to the presence of the turbulence. This irregularity is not important until it begins to obscure the arrival of the front. What seems to happen in practice is that if a probe is positioned in a particular flow, such as the reverse flow region behind a bluff body, and the mainstream speed is increased from zero, the sensor-wire signals begin by being very similar to those obtained in steady flow although the times of flight fluctuate considerably. As the Reynolds number is increased, the signal amplitudes diminish, as would be expected from the results of § 4.2, and, as the extent of the turbulence spectrum increases, the irregularity in the sensor-wire signals becomes more marked until a point is reached when the signals are so irregular that estimations of the times of flight are no longer possible. Numerous attempts have been made to estimate this effect theoretically assuming local isotropy of the small eddy structure. But, it has proved more difficult than one might expect to explain the observed behaviour of the probe, and, apart from the conclusion that it is best to have the largest scale of flow possible for a given Reynolds number, the results of the analysis have not been very useful. However, from a practical standpoint it seems possible with the normal scale of wind-tunnel experiments to obtain reasonable signals although it is clearly an advantage to have the scale of the experiments as large as the facilities will allow.

A number of examples of measurements with the pulsed hot-wire anemometer have now been published but, as a single example of the type of measurement that can now be made, figure 19 shows a comparison between pulsed-wire and linearized hot-wire measurements of mean velocity along the centre-line of the flow downstream of a circular cylinder and also an 18:1 tapered circular cylinder. These results were the first measurements made with the pulsed-wire probe

(Bradbury 1969) and, for a variety of reasons, they are perhaps the least satisfactory. However, they serve to illustrate the essential feasibility of the instrument for making measurements in flow regions where the hot-wire anemometer is subject to gross errors.

Tombach (1969) used the intercept technique for measurements with a cross-wire probe in a turbulent jet of foreign gas. There are a number of important differences between his work and the present investigations but the main one seems to be that the turbulence scale in his experiments was too small compared with the probe dimensions to give clear individual traces. As a consequence, the sensor-wire signals were digitized and an 'average' sensor-wire signal obtained on a computer. However, if this is done, the instrument immediately becomes highly non-linear and, in particular, estimates of the turbulent intensity become extremely difficult to make.

6. A system for the automatic measurement of the flight times

Measurements of the intercept positions from an oscilloscope are convenient only if there are a limited number of measurements to be made. An alternative scheme to speed up data aquisition has been studied using differentiated wire signals along the lines discussed in § 2.4. The complete circuitry of the system is shown in figure 9. Although this circuit may seem fairly formidable it took only a short while to develop using a modular instrumentation system developed by B. J. Belcher in the Aeronautics Department at Imperial College. This system used operational amplifiers and a variety of logic integrated circuits built into a range of modules with patch board front panels. These may be readily interconnected, and it is possible to build up fairly sophisticated systems without too much development work.

The basic sensor-wire signal is first amplified and differentiated, see the first inset diagram in figure 9. Because of the subsequent deterioration in signal-to-noise ratio, it is necessary to pass the resulting signal through a low pass filter set at about 10 kHz. As a result of both the differentiation and the filtering, the pick-up signal from the pulsed wire at the beginning of the sensor-wire trace is considerably longer than the original pulse, and it has a decay time constant typically of the order of 100 μsec. The differentiated signal is then fed to two comparators which are set to trigger at a voltage of about a half the maximum value of the differentiated signal. As discussed earlier, the setting of the comparator trigger level is not too critical. The comparators are set to trigger off signals of opposite polarity so that outputs are obtained irrespective of the flow direction. In addition to the signal from the heat pulse, the comparators are also triggered by the initial pick-up signal so that the signals from the comparators are similar to the two lower traces shown in the second inset diagram in figure 9. The comparator outputs arising from the electrical pick-up signal are eliminated by passing the comparator outputs through two AND gates which are initially blanked off by a pulse of about 100 μsec duration, and which is produced from the pulse generator at the same time as the heat-tracer pulse is fired. Signals similar to those shown in the third inset diagram in figure 9 are then obtained.

These two AND gate outputs are then fed into two RS Flip Flops which produce step-like signals with a duration equal in length to the time from the firing of the heat-tracer pulse to the arrival of a signal at the sensor wires sufficient to trigger the two comparators. Both comparators may be triggered by the heat-tracer signal from the one sensor wire because the differentiated sensor-wire signal swings both positively and negatively, but it is obviously the shorter of the two times which corresponds to the desired time of flight. The selection of the shorter time step is obtained by passing the flip-flop outputs through an OR gate (fourth

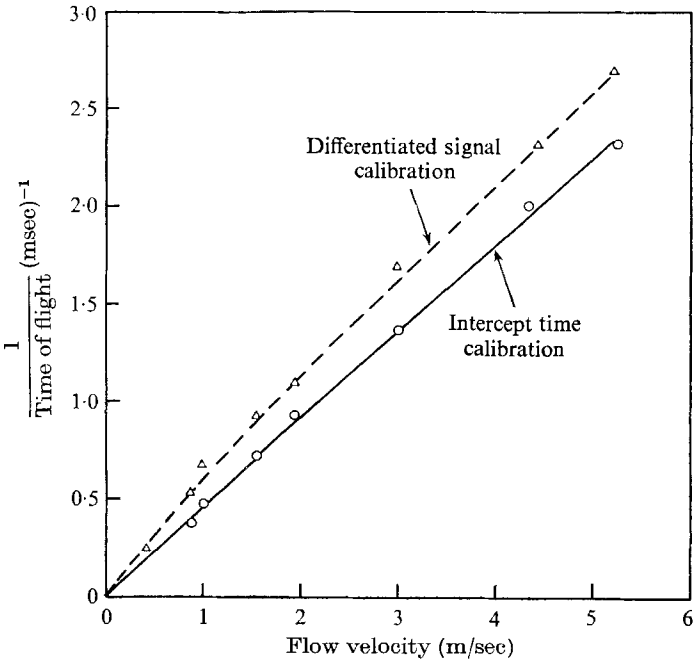

FIGURE 22. Comparison between a differentiated signal calibration and an intercept time calibration.

diagram in figure 9). The OR gate output is then fed through an operational amplifier with an accurately clamped maximum output voltage level so that it gives a pulse of fixed amplitude with a duration equal to the time of flight. This is fed to an integrator which produces a ramp whose final amplitude is proportional to the time of flight. This is then passed through a switched amplifier which produces a final output with a polarity dependent on which of the two comparators is triggered first. The fifth diagram in figure 9 shows the two types of switched amplifier output that can occur – one in which the integrator polarity is correct and the other where the polarity is switched on the arrival of the heat pulse. Therefore, the final output is a d.c. voltage whose amplitude is proportional to the time of flight and whose polarity gives the flow direction. In the present arrangement, this voltage is displayed on a digital voltmeter and the value punched out on paper tape.

Figure 22 shows a calibration from a differentiated sensor-wire signal compared

with the intercept time calibration. The calibration is now slightly curved as would be expected from the theoretical arguments in § 2.4. But, this slight non-linearity can be removed in the subsequent computation of the velocities.

Numerous measurements have now been made with this automatic system in a variety of flows and they confirm the usefulness of the technique in studying highly turbulent flows. It is, of course, possible to set up different circuitry to automatically measure the time of flight and the precise choice is probably best dictated by what type of instrumentation is available to the experimenter.

7. Concluding remarks

This paper has described the results of both theoretical and experimental investigations into a pulsed-wire probe using a time-of-flight technique for velocity measurements. The technique seems to have considerable potential for exploring highly turbulent flows which hitherto have not been amenable to proper experimental investigation. However, although the present work represents a start on the development of the technique, it is clear that there are many aspects of the probe behaviour that requires further investigation. These include the yaw response, the influence of the pulsed-wire wake and the general behaviour of the probe at very low Péclet numbers. Also, there is clearly a need for developing the technique in a form which makes it simpler to use. The particular system explored in the present work is clearly workable, but other techniques perhaps along the lines suggested in § 2.4 should also be investigated.

In addition to the applications described in this paper, the technique could also be used in gas mixtures and, in fact, Mcquaid & Wright (1971) have already made an interesting application of the pulsed-wire probe to measurements in a low turbulence level flow of variable density. Another possible application is to use two probes for more elaborate spatial and temporal correlation measurements.

There are, of course, other techniques which are being developed for use in highly turbulent flows. Multiple hot-wire arrays could possibly be used although the 'untangling' of the results might require a prohibitive effort. Also, the accuracy of hot-wire anemometer measurements depends on a sensitive 'analog' calibration whereas the pulsed-wire calibration depends only on the probe geometry – it is very nearly a 'digital' instrument. In addition, the application of laser Doppler techniques for velocity measurement are currently being studied. But, although the potential of these techniques is considerable, they involve a high degree of sophistication in instrumentation and, for many applications, the use of a somewhat simpler technique such as the pulsed-wire probe may be more appropriate.

Appendix. Errors due to the finite yaw response of a pulsed-wire probe

For a normally distributed isotropic turbulence, the joint probability density function is

$$f(u,v,w) = \frac{1}{(2\pi\overline{u^2})^{\frac{3}{2}}} \exp\left[\frac{-(u-U)^2-v^2-w^2}{2\overline{u^2}}\right].$$

The probability of missing a tracer is

$$p = 1 - \iiint_{\text{cones}} f(u, v, w)\, du\, dv\, dw,$$

where the integration is restricted to the two cones on either side of the pulsed wire within which the sensor wires will pick up signals. If we introduce a radial velocity $v_r = (v^2 + w^2)^{\frac{1}{2}}$ inclined at an angle ψ to the xy plane, we have

$$v = v_r \sin\psi, \quad w = v_r \cos\psi.$$

For the downstream cone with a half angle ϕ, this change of co-ordinates gives

$$I_{dl} = \iiint_{\substack{\text{downstream} \\ \text{cone}}} f(u, v, w)\, du\, dv\, dw$$

$$= \frac{1}{(2\pi\overline{u^2})^{\frac{3}{2}}} \int_0^{\infty} \left[\int_0^{u\tan\phi} \int_0^{2\pi} v_r \exp\left[\frac{-(u-U)^2 - v_r^2}{2\overline{u^2}} \right] d\psi\, dv_r \right] du.$$

It should be noted that the upper limit on the integration with respect to v_r is $u\tan\phi$ which ensures that the integration is limited to the downstream cone. The evaluation of this integral is straightforward (see Castro 1970) and it gives

$$I_d = \frac{1}{2}\left(1 + \operatorname{erf}\frac{U}{(2\overline{u^2})^{\frac{1}{2}}}\right) - \tfrac{1}{2}\cos\phi \exp\left[-\frac{\sin^2\phi}{2(\overline{u^2}/U^2)} \right] \left(1 + \operatorname{erf}\frac{U\cos\phi}{(2\overline{u^2})^{\frac{1}{2}}}\right).$$

The integral for the upstream cone is obtained by writing $-U$ for U in this expression and the probability of missing a tracer then reduces to

$$p = \cos\phi \exp\left[\frac{-\sin^2\phi}{2(\overline{u^2}/U^2)} \right]$$

which is equation (20) in the main text.

The measured mean velocity including the missed tracers as zero velocity results is given by

$$U_m = \iiint_{\text{cones}} uf(u, v, w)\, du\, dv\, dw.$$

The measured intensity including the missed tracers is given by

$$\overline{u_m^2} = \iiint_{\text{cones}} (u - U_m)^2 f(u, v, w)\, du\, dv\, dw + pU_m^2$$

$$= \iiint_{\text{cones}} u^2 f(u, v, w)\, du\, dv\, dw - U_m^2,$$

where it should be noted that the intensity is evaluated relative to the estimated mean velocity and not to the true mean velocity. This seems a more consistent approach to adopt. The evaluation of these integrals is tedious but it results finally in the expressions given in the main text as equations (21) and (22).

REFERENCES

BAUER, A. B. 1965 Direct measurement of velocity by hot wire anemometry. *A.I.A.A. J.* **3**, 1189.

BRADBURY, L. J. S. 1969 A pulsed-wire technique for velocity measurements in highly turbulent flows. *NPL Aero Report* 1284.

BRADBURY, L. J. S. & CASTRO, I. P. 1971 Some comments on heat transfer laws for fine wires. *J. Fluid Mech.* To be published.

CASTRO, I. P. 1970 The pulsed wire anemometer – an analysis to determine the errors caused by the probe finite yaw response. *Imperial College Aeronautics Dept. Report.*

CASTRO, I. P. 1971 Wake characteristics of two-dimensional perforated plates normal to an airstream. *J. Fluid Mech.* **46**, 599.

COLLIS, D. C. & WILLIAMS, N. J. 1959 Two-dimensional convection from heated wires at low Reynolds numbers. *J. Fluid Mech.* **6**, 357.

MANDEL, J. 1964 *The statistical analysis of experimental data.* New York: Interscience.

MCQUAID, J. & WRIGHT, W. 1971 The measurement of fluctuating velocities in flows of gas mixtures using a pulsed wire anemometer. To be published.

TOMBACH, I. H. 1969 Velocity measurements with a new probe in inhomogeneous turbulent jets. Ph.D. thesis, California Institute of Technology.